Neuropsychiatric Disease and Treatment

Dovepress

open access to scientific and medical research

Open Access Full Text Article

ORIGINAL RESEARCH

Electroacupuncture Promoting Axonal Regeneration in Spinal Cord Injury Rats via Suppression of Nogo/NgR and Rho/ROCK Signaling Pathway

This article was published in the following Dove Press journal:
Neuropsychiatric Disease and Treatment

Wei-Ping Xiao[1,*]
Li-Li-Qiang Ding[2,*]
You-Jiang Min[1,3]
Hua-Yuan Yang[4]
Hai-Hua Yao[3]
Jie Sun[1]
Xuan Zhou[1]
Xue-Bo Zeng[1]
Wan Yu[1]

[1]Spinal Department of Orthopedics and Department of Acupuncture, Affiliated Hospital of Jiangxi University of Traditional Chinese Medicine, Nanchang, Jiangxi, People's Republic of China; [2]Department of Hypertension, Shanghai Institute of Hypertension, Ruijin Hospital, Shanghai Jiao Tong University School of Medicine, Shanghai, People's Republic of China; [3]Department of Traditional Chinese Medicine, Shanghai Eighth People's Hospital, Shanghai, People's Republic of China; [4]Institute of Traditional Chinese Medicine Engineering, Shanghai University of Traditional Chinese Medicine, Shanghai, People's Republic of China

*These authors contributed equally to this work

Purpose: To observe the changes of Nogo/NgR and Rho/ROCK signaling pathway-related gene and protein expression in rats with spinal cord injury (SCI) treated with electroacupuncture (EA) and to further investigate the possible mechanism of EA for treating SCI.

Methods: Allen's method was used to create the SCI rat model. Sixty-four model rats were further subdivided into four subgroups, namely, the SCI model group (SCI), EA treatment group (EA), blocking agent Y27632 treatment group (Y27632) and EA+blocking agent Y27632 treatment group (EA+Y), according to the treatment received. The rats were subjected to EA and/or blocking agent Y27632 treatment. After 14 days, injured spinal cord tissue was extracted for analysis. The mRNA and protein expression levels were determined by real-time fluorescence quantitative PCR and Western blotting, respectively. Cell apoptosis changes in the spinal cord were evaluated by in situ hybridization. Hindlimb motor function in the rats was evaluated by Basso-Beattie-Bresnahan assessment methods.

Results: Except for RhoA protein expression, compared with the SCI model group, EA, blocking agent Y27632 and EA+blocking agent Y27632 treatment groups had significantly reduced mRNA and protein expression of Nogo-A, NgR, LINGO-1, RhoA and ROCK II in spinal cord tissues, increased mRNA and protein expression of MLCP, decreased p-MYPT1 protein expression and p-MYPT1/MYPT1 ratio, and caspase3 expression, and improved lower limb movement function after treatment for 14 days ($P<0.01$ or <0.05). The combination of EA and the blocking agent Y27632 was superior to EA or blocking agent Y27632 treatment alone ($P < 0.01$ or <0.05).

Conclusion: EA may have an obvious inhibitory effect on the Nogo/NgR and Rho/ROCK signaling pathway after SCI, thereby reducing the inhibition of axonal growth, which may be a key mechanism of EA treatment for SCI.

Keywords: Nogo/NgR, Rho/ROCK, MLCP, MYPT1, spinal cord injury, Y27632, electroacupuncture

Correspondence: You-Jiang Min
Shanghai Eighth People's Hospital, Caobao Road 8, Shanghai 200235, People's Republic of China
Tel +86 18221786381
Email myj2002@126.com

Hua-Yuan Yang
Shanghai University of Traditional Chinese Medicine, Cairen Road 1200, Shanghai 201203, People's Republic of China
Tel +86 13651968830
Email yhyabcd@sina.com

Introduction

Traumatic paraplegia caused by spinal cord injury (SCI) is a severe neurological injury that often leads to profound disability,[1–3] and SCI results in high mortality and mutilation.[4] With the recent, rapid development of traffic, architecture and mining, the number of patients suffering from SCI, most of whom are middle-aged or young men, has increased yearly, and SCI imposes a heavy burden on people's productiveness and livelihood as well as on a country's economy.[2,5,6] According to statistics from the USA, the average expenditure for therapeutic rehabilitation of

each SCI patient exceeds 750 thousand dollars in his/her lifetime, and the total expenditures for SCI patients exceed 6 billion dollars in the United States every year.[7] To date, there is no effective pharmacological or methodological treatment for SCI in modern medicine.[8]

Recently, clinical reports have indicated that electroacupuncture (EA) is widely used to treat SCI and has been shown to be beneficial for recovery from SCIs, especially incomplete paraplegia.[9–12] Moreover, EA has a better curative effect with respect to improving bladder and bowel function, ameliorating limb spasm and relieving neurological pain, which are caused by SCI.[9,10,12] However, the exact mechanisms remain to be fully elucidated.

Several lines of evidence suggest that the signaling pathway of the Nogo protein/Nogo protein receptor (NgR) and the ras homolog gene/Rho-associated coiled coil-forming protein kinase may play a key role in mediating the regeneration of neurons and axons in the adult central nervous system (CNS) after SCI.[13,14] Extracellular inhibitory signaling factors, such as myelin-associated glycoprotein (MAG), Nogo protein, and oligodendrocyte myelin glycoprotein (OMgp), further initiate intracellular signal transduction by the transmembrane protein NgR.[15] NgR and the cooperative receptor p75NTR (p75 neurotrophin receptor) compose the NgR/p75NTR coordinative body. This body and LINGO-1 (leucine-rich repeat Ig domain-containing Nogo-interacting protein 1) together constitute a receptor complex via a ternary complex of NgR/LINGO-1/p75NTR, which activates the intracytoplasmic signal.[16–18] After the combination of Rho-GPI (glycosyl phosphatidyl inositol, GPI) and p75NTR, RhoA, which is released from the inhibition of Rho-GPI, following activated Rho factor, causes inactive Rho-GDP to change into Rho-GTP. Rho-GTP further activates ROCK which influences its substrate myosin light chain (MLC) by causing MLC phosphorylation. Meanwhile, activated ROCK can also promote the phosphorylation of myosin phosphatase target subunit 1 (MYPT1), a subunit of MLC phosphatase (MLCP), and then promote the autochthonous activity of MLCP, which inhibits the dephosphorylation of MLC and indirectly increases the phosphorylation level of MLC.[19,20] Phosphorylated MLC can stimulate the combination of myosin and actin, trigger contraction of myosin, and then influence the structure of the cytoskeleton, causing neuronal apoptosis, which results in limited regeneration of neural axons.[21–23] Micromolecule Y27632, a specific inhibitor of ROCK II, not only can inhibit the activities of ROCK but can also block the role of chondroitic acid proteoglycan and then promote neural axon growth, injured CNS axon growth and functional recovery.[24,25]

Previous studies indicate that acupuncture could treat SCI by regulating the gene and protein expression of Nogo-A, NgR and/or RhoA, ROCK II.[26–28] Does EA influence the Nogo/NgR and Rho/ROCK signal pathway after SCI? How does EA treat SCI by affecting the Nogo/NgR and Rho/ROCK signaling pathway?

Materials and Methods

Experimental Animals

Eighty healthy, clean, female, Sprague Dawley (SD) rats aged 8 weeks (weighing 200 ± 20 g) were purchased from the Slack-Jingda Laboratory Animals Co., Ltd., of Hunan Province, China (certificate no. SCXK (Xiang) 2011–0003). The rats were fed with standard fodder and with food and water freely available in a controlled environment with a constant temperature of 20~25°C and a 12/12-hr light/dark cycle.[28] Following a 3-day adaptation, all rats were begun to experiment.[28] All procedures were conducted in accordance with guidelines reviewed and approved by the Institutional Animal Care and Use Committee of Jiangxi University of Traditional Chinese Medicine, China[28]. Female animals are routinely used in SCI studies because female animals allow for easier manual expression of bladders after SCI, less urinary tract infection, and less mortality.[23] In addition, there are reports showing that no significant differences were detected in histological and behavioral outcomes between male and female animals after SCI.[29]

Modeling

Eighty rats were randomly divided into two groups: sham operation (sham, n=16) and model establishment (model, n = 64). Models of SCI were established in accordance with published methods.[30] All rats were anesthetized with 3% pentobarbital sodium (1.5 mL/kg, Sigma, USA) intraperitoneally and an incision made.[31] The T_{10} vertebral body of each rat was located by counting the ribs. The T_{10} vertebral lamina was removed by rongeur forceps to expose the spinal cord completely. Sixty-four rats were induced by striking the spinal cord with an electric cortical contusion impactor. Strike parameters consisted of a strike tip with a diameter of 3 mm, velocity of 5 m/s, retention time of 0.5 s and compression of 1.5 mm.[31] The criterion for successful model creation was one of three conditions below: rapid accumulation of edema and stagnant blood at the

trauma site in the dura mater of the spinal cord, accompanied by rat tail spastic swinging, contractive vibration of the hind limb, or convulsive tics of the rat body.

The spinal process at the L_5-S_1 joints was removed using the same method mentioned above, and the spinal cord was exposed. A small hole was made on the surface of the dura mater of the spinal cord with microscissors, avoiding the median vessel. A PE 10 hose was clamped and pressed under the dura mater and inserted into the arachnoid cavity slowly if clear cerebrospinal fluid was seen to overflow from the outside of the catheter, indicating that catheterization was successful. The hose was fixed onto the fascia by a surgical suture, with the reveal port approximately 1 cm away from the skin; the reveal port was closed with a guide wire to prevent the overflow of cerebrospinal fluid.[31] The wound was washed with saline and penicillin, and the injured rats were raised in separate cages.

Sham operation control animals received laminectomy only. All model rats received an intra-muscular penicillin injection twice a day, followed by suturing of the incision. Manual bladder expression was carried out at least 3 times daily until reflex bladder emptying was established.

Grouping and Treatment

After being evaluated for hindlimb motor function by the Basso-Beattie-Bresnahan (BBB) method, sixty-four model rats were randomly subdivided into an SCI model group (SCI, n=16), EA treatment group (EA, n = 16), blocking agent Y27632 subdural injection treatment group (Y27632, n = 16), and EA plus blocking agent Y27632 subdural injection treatment group (EA+Y, n = 16). All rats were restrained with the same method and all treatments were started at 7 days following SCI.[31]

In the EA treatment group, the rats were restrained on a board. Stainless steel 0.18-mm-diameter needles (*Hwato* Disposable Acupuncture Needle; Jiangsu Medical Supplies Factory, Jiangsu Province, China) were inserted to a depth of approximately 5 mm at the following acupoints: *Yaoyangguan* (GV3, posterior midline and in the depression below the spinous process of the fourth lumbar vertebra), *Dazhui* (GV14, posterior midline and in the depression below the spinous process of the seventh cervical vertebra) and *Zusanli* (ST36, bilaterally on hindlimbs below the fibular head 5 mm), *Ciliao* (BL32, corresponding to the second sacral posterior) on both sides.[32] Then, the needles were connected to an *Hwato* SDZ-II EA apparatus (Suzhou, Jiangsu Province, China). Alternating strings of dense-sparse frequencies (100 Hz for 1.5 ms and 2 Hz for 1.5 ms alternately) were selected. The intensity was adjusted to induce a slight twitch of the hindlimb (the electric current wave width was 4 ms, and the output voltage was 2 V). EA treatment was performed for 20 mins once per day, lasting for 14 days. After EA treatment, the rats were given normal saline by subdural injection via a microinjector from a homemade PE10 tube, each rat received 0.54 mL/kg, once per day, lasting for 14 days.[31]

Rats in the Y27632 treatment group received the blocking agent Y27632 (Qilu Pharmaceutical Co., Ltd., Jinan, Shandong Province, China) by subdural injection via a microinjector from a homemade PE10 tube (18 μg Y27632 lyophilized powder was dissolved in 30 μL phosphate buffered saline solution; each rat received 0.54 mL/kg), once per day, lasting for 14 days.[31]

Rats in the EA+Y treatment group received both EA and Y27632 subdural injection treatment.

Rats in the sham operation group and the SCI model group were received normal saline by subdural injection according to the methods mentioned above.

Behavioral Assessments

The BBB scores were on a scale of 0 to 21 (21 normal locomotion, 0 complete hind limb paralysis), which is based on hind limb movements made in an open field. The BBB Scale locomotor tests of all rats were blindly performed before treatment and on the 7th and 14th day when treatment began by 2 trained observers lacking knowledge of the experimental groups, according to a method published previously.[28] Before assessment, the bladder of each rat was emptied to avoid abnormal behavior caused by a full bladder. Briefly, rats were placed in an open field and observed for 3 mins. Each rat was evaluated 3 times, and the average integer value was recorded.[31]

Sampling

Eight rats in each group were randomly sacrificed at 14 days after treatment; four rats from each group were used for real-time quantitative polymerase chain reaction (RT-qPCR) and the remaining four rats were used for a Western blot assay.

After the treatment, 8 rats in each group were randomly selected to be anesthetized with 3% pentobarbital sodium (1.5 mL/kg) intraperitoneally. After the rats were deeply anesthetized, the thoracic cavity was exposed and the heart was fully exposed. The blunt tip of the gavage needle was inserted into the aorta from the left ventricle, and the right heart ear was cut open. Approximately 150 mL of 0.9% normal saline was infused when the liver color was

grayish white and the fluid from the heart changed from red to transparent and clear. The perfusion was stopped until the rats' limbs twitched or the whole body was stiff and the liver became hard. The perfusion of a 4% paraformaldehyde solution was approximately 350 mL in volume and lasted for approximately 2 hrs. A 10-mm spinal cord segment containing the injury epicenter was isolated from each animal and soaked in the 4% paraformaldehyde solution for storage.[31] In addition, the remaining rats in each group were sacrificed with decapitation, and on an ice tray, a 10-mm spinal cord segment containing the injury epicenter was isolated from each animal. Then, the tissues were placed in liquid nitrogen for freezing and finally transferred into a −80°C refrigerator for preservation.

Reverse Transcription Real-Time Quantitative Polymerase Chain Reaction (RT-qPCR)

RT-qPCR was performed using the SYBR Green system. Total RNA was isolated from the spinal cords of rats in each group using Trizol solution (Invitrogen, Carlsbad, CA, USA). The mRNA expression levels of Nogo-A, NgR, LINGO-1, RhoA, ROCK II and MLCP were measured using an RT-qPCR system with SYBR Green (Thermo Fisher Scientific, Waltham, MA, USA). cDNA was amplified by PCR using primers for each target gene. RT-qPCR conditions were as follows: 94°C for 5 mins, followed by 40 cycles of 95°C for 15 seconds, 60°C for 45 seconds and 72°C for 30 seconds. The fluorescence signal was detected at 60°C, and the samples were finally extended at 72°C for 7 mins. The amplification efficiency was compared between the target and reference control glyceraldehyde 3-phosphate dehydrogenase (GAPDH) using the delta-delta Ct (ΔΔCt) method.[33] The primers employed are listed in Table 1.

Western Blot Assay

Western blot analysis was performed as described previously with minor modifications.[28] All spinal cord tissues obtained in each group were homogenized in lysis buffer (JRDUN Biotechnology, Shanghai, China). Equal amounts of proteins were separated by sodium dodecyl sulfate-polyacrylamide gel electrophoresis (SDS-PAGE), and then the resolved proteins were transferred to polyvinylidene fluoride (PVDF) membranes (Millipore, Bedford, MA, USA). The membranes were incubated with primary antibodies overnight at 4°C. Monoclonal antibodies used for Western blotting included a rat monoclonal anti-Nogo-A antibody (1:1000; Santa Cruz Biotechnology, Santa Cruz, CA, USA). The antibodies used in this study were rat monoclonal antibodies, 1:1000 and were purchased from Santa Cruz Biotechnology (Santa Cruz, CA, USA), except for those specifically indicated. The other antibodies included anti-NgR, anti-LINGO-1, anti-RhoA, anti-ROCK II, anti-MLCP, anti-MLC, anti-p-MLC and anti-GAPDH. The membranes were washed 5 mins with Tris-buffered saline Tween 3

Table 1 Primer Sequences for Real-Time Quantitative Polymerase Chain Reaction

Gene	Full Name	Sequences (5–3′)	Product Size (bp)
Nogo-A	Nogo A	Sense primer: GGT GCC TTG TTC AAT GGT C antisense primer: AAT CTG CTT TGC GCT TCA	183
NgR	Nogo protein receptor	Sense primer: AGA AAG AAC CGC ACC CGT AG antisense primer: GGC CCA AGC ACT GTC CAA	155
LINGO-1	Leucine rich repeat and Ig domain containing 1	Sense primer: GCT GAC GCT GGA GAA ATG antisense primer: GAA GGA GTA GTC CCG TAT GG	109
RhoA	Ras homolog family member A	Sense primer: GAT GGA GCT TGT GGT AAG antisense primer: ATC AGT GTC TGG GTA GGA G	150
ROCK II	Rho-associated kinase II	Sense primer: ATC TCA TTT GTG CCT TCC antisense primer: CTG GTG CTA CAG TGT CTC G	143
MLCP	Myosin light chain phosphatase	Sense primer: GCT CCC ACC TTC TGT TTG antisense primer: CGA CGG CTT TCA TACTCC	234
GAPDH	Glyceraldehyde 3-phosphate dehydrogenase	Sense primer: GCA AGT TCA ACG GCA CAG antisense primer: GCC AGT AGA CTC CAC GAC AT	146

times and incubated with goat anti-rabbit IgG-HRP (1:1000; Beyotime Biotechnology, Shanghai, China) and goat anti-mouse IgG-HRP PS1 (C-20) (1:1000; Beyotime Biotechnology, Shanghai, China) antibodies at 37°C for 1 hr. The immunoreactive bands were visualized using an enhanced chemiluminescence reagent (Beyotime Biotechnology, Shanghai, China). The grayscale values of bands were quantified using ImageJ software (Fujifilm, Tokyo, Japan). The relative expression of protein was calculated based on the ratio of target grayscale values to loading control grayscale values.

In situ Hybridization

Spinal cord segments containing the epicenter were isolated from each animal and embedded with paraffin. Four paraffin blocks were selected randomly and placed into a refrigerator at −20°C for at least 30 mins. Then, the blocks were cut into 4–7-μm-thick serial sections.

The sections were deparaffinized with xylene 3 times for 5 mins per time. The xylene was removed in a gradient of 100%, 96% and 70% alcohol. The sections were air dried, washed for 2–5 mins with PBS, and subjected to removal of proteases and dehydration in gradient alcohol. Each section was incubated in 50 μL hybridization buffer containing 10 μM oligonucleotide probe at 95°C for 5 mins and 37–40°C for 12 hrs, washed three times with 5×, 1× and 0.2× saline sodium citrate, and treated with blocking buffer at 37°C for 15 mins. Then, the blocking buffer was blotted with paper. Each section was then incubated in 30 μL biotinylated anti-digoxin antibody (1:50) at 37°C for 1 hr, washed four times with 0.5 M PBS, incubated in streptavidin-biotin-peroxidase complex at 37°C for 30 mins, and rinsed four times in 0.5 M PBS. Subsequently, the sections were developed in 3, 3, diaminobenzidine, counterstained with hematoxylin, dehydrated in alcohol, permeabilized in xylene, mounted with proof quench mounting agent, and photographed with a fluorescence microscope.[34] The morphology of nerve cells in the spinal cord was observed under a microscope. The upper, middle, lower, left and right visual fields were randomly selected for each section, and the positive cells were counted. Image-Pro Plus 6.0 software was used to count the positive cells, and the mean value was finally taken for statistical analysis. Negative controls were incubated in 0.01 M PBS without primary antibody. The primers employed are shown in Table 2.

Statistical Analyses

All data are presented as the mean±SD. Data were analyzed by one-way analysis of variance followed by a post hoc Student-Newman-Keuls (SNK) test using SPSS 17.0 software (SPSS, Chicago, IL, USA). A value of $P<0.05$ was considered statistically significant.

Results

BBB Scores

The BBB score of each group at 2 time points postinjury was 0 before treatment, and no hind limb movement was observed in each group of rats, indicating that the model for SCI was successful. After 14 days of treatment, compared with the SCI model group, the BBB score in each treatment group was significantly increased ($P<0.01$), and there was no significant difference between the EA treatment group and the Y27632 treatment group ($P > 0.05$). However, the BBB score in the EA+Y27632 treatment group was higher than those in the EA treatment group and the Y27632 treatment group ($P<0.01$), as shown in Figure 1.

The Protein Expression of Nogo-A, NgR and LINGO-1 by Western Blotting

The relative protein expression levels of Nogo-A, NgR and LINGO-1 in the SCI model group were significantly higher than those in the sham operation group ($P<0.01$ or < 0.05). After EA treatment, the Nogo-A, NgR and LINGO-1 relative protein expression levels were significantly decreased compared with those in the SCI model group ($P < 0.01$ or < 0.05), as shown in Figure 2.

The mRNA Expression of Nogo-A, NgR and LINGO-1 by qRT-PCR

The relative mRNA expression levels of Nogo-A, NgR and LINGO-1 in the SCI model group were

Table 2 Primer Sequences for Hybridization in situ

Gene	Sequences (5′–3′)
Caspase3	CAGCGTCGGCATCGTCTACAAGCACTAGATGAGCGTCCTGCACATGGACGTCATGGCAGAGTACATGCTGAGTGTCAATT CCACGGGGCACATGGAGAACATATTTGACTTCCGCCTCGCAAGTAGGTAT

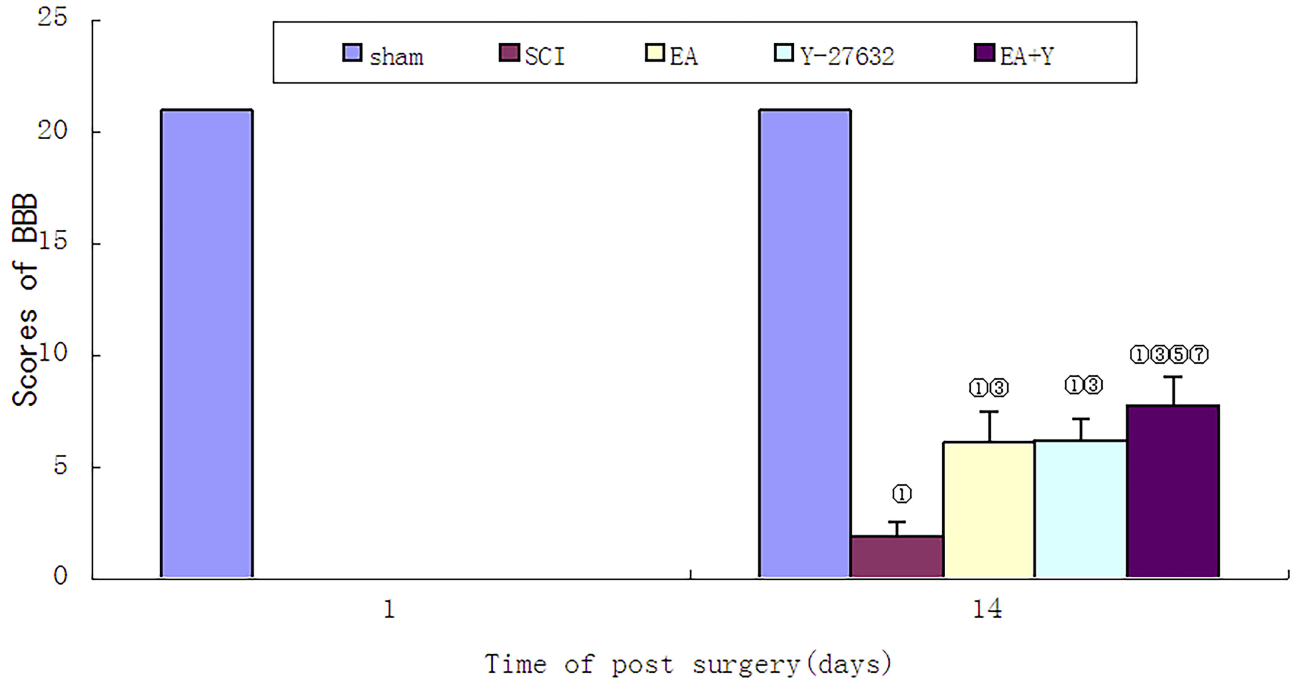

Figure 1 BBB score of each group before treatment and on the 14th days. ① P< 0.01, ② P<0.05 versus sham; ③ P<0.01, ④ P<0.05 versus SCI; ⑤ P<0.01; ⑥ P<0.05 versus EA; ⑦ P<0.01; ⑧P<0.05 versus Y27632. Data are expressed as the mean±SD (1-way analysis of variance and Student-Newman-Keuls post hoc test, n=8 rats/group).
Abbreviations: sham, sham operation; SCI, spinal cord injury; EA, electroacupuncture; Y, blocking agent Y27632.

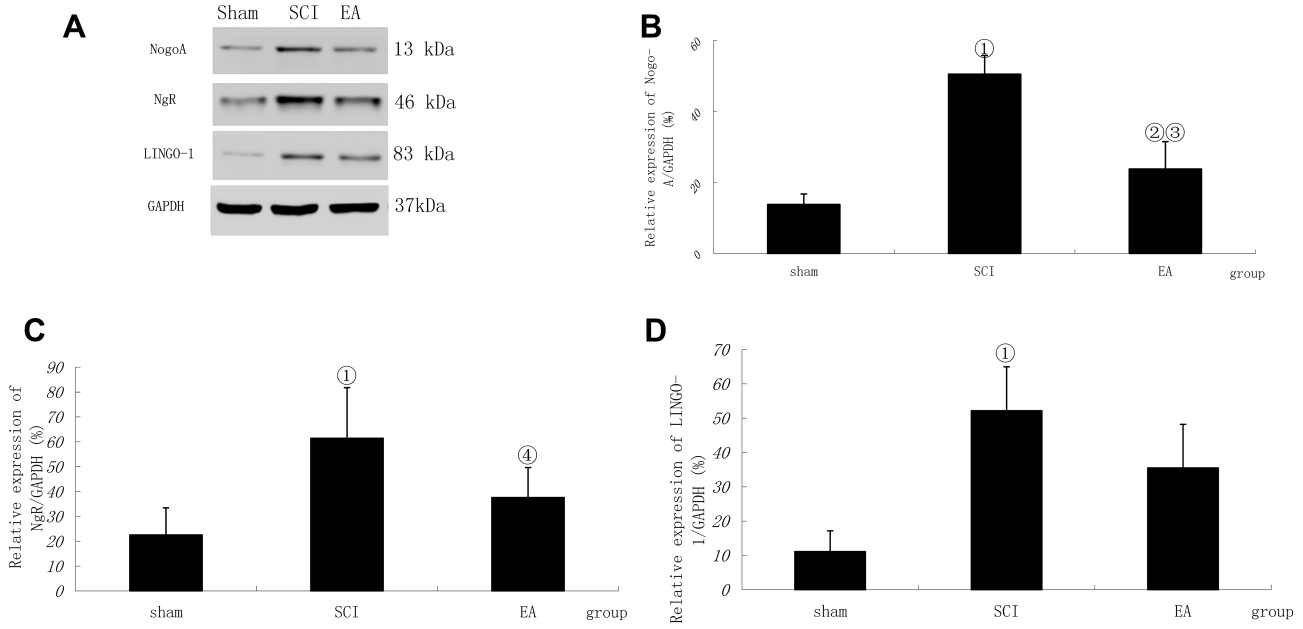

Figure 2 Nogo-A, NgR and LINGO-1 activation following SCI. (**A**) Western blotting bands for Nogo-A, NgR and LINGO-1. Compiled results in a bar graph for the relative protein expression (**B**) of Nogo-A. (**C**) of NgR. (**D**) of LINGO-1. ① P < 0.01, ② P<0.05 versus sham. ③ P<0.01, ④ P<0.05 versus SCI. Data are shown as the mean ±standard error of the mean (1-way analysis of variance and Student-Newman-Keuls post hoc test, n=4 rats/group).
Abbreviations: sham, sham operation; SCI, spinal cord injury; EA, electroacupuncture.

significantly higher than those in the sham protein group (P < 0.01 or < 0.05). After EA treatment, the Nogo-A, NgR and LINGO-1 relative mRNA expression levels were significantly decreased compared with those in the SCI model group (P < 0.01 or < 0.05), as shown in Figure 3.

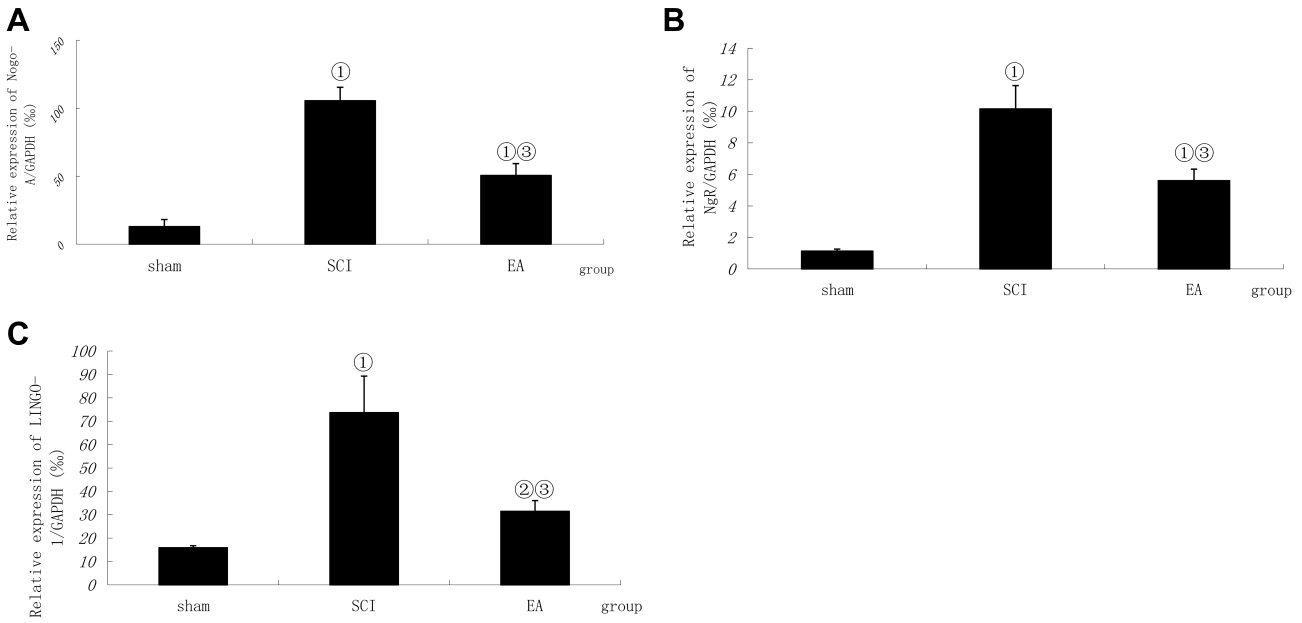

Figure 3 Comparison of the mRNA relative expression of Nogo-A, NgR and LINGO-1. Compiled results in a bar graph for the relative mRNA expression (**A**) of Nogo-A. (**B**) of NgR. (**C**) of LINGO-1. ① P < 0.01, ② P<0.05 versus sham. ③ P<0.01. Data are shown as the mean±standard error of the mean (1-way analysis of variance and Student-Newman-Keuls post hoc test, n=4 rats/group).
Abbreviations: sham, sham operation; SCI, spinal cord injury; EA, electroacupuncture.

The Protein Expression of RhoA, ROCK II and MLCP by Western Blotting

The expression of MLCP in the SCI model group was noticeably lower than that in the sham operation group (P<0.01); in contrast, the expression levels of ROCK II and RhoA in the SCI model group were significantly higher than those in the sham operation group (P<0.01). After EA treatment, the expression of MLCP was significantly increased compared with that in the SCI model group (P<0.05), and the ROCK II protein expression was significantly decreased (P<0.05). In contrast, the RhoA protein expression was not significantly decreased (P>0.05). After treatment with the blocking agent Y27632, compared with the SCI model group, the treatment group showed the same change tendency in MLCP, ROCK II and RhoA protein expression with EA treatment (P<0.05; P<0.01; P>0.05). After treatment with EA plus the blocking agent Y27632, the MLCP protein expression was significantly higher than that in the SCI model group (P<0.05), while the ROCK II and RhoA protein expression levels were significantly lower than those in the SCI model group (P<0.01 or <0.05). Comparison between EA and Y27632 treatment revealed that the protein expression levels of MLCP, ROCK II and RhoA were not significantly different (P>0.05). After treatment with EA plus the blocking agent Y27632, compared with the corresponding expression levels after EA treatment, the MLCP protein expression was significantly increased (P<0.05), the ROCK II protein expression was significantly decreased (P<0.05), and the RhoA protein expression was not markedly decreased (P>0.05). Compared with the corresponding expression levels after Y27632 treatment, the protein expression levels of MLCP increased significantly (P<0.05); by contrast, the ROCK II and RhoA protein expression levels were not markedly decreased (P>0.05), as shown in Figure 4.

The mRNA Expression of RhoA, ROCK II and MLCP by qRT-PCR

The mRNA expression of MLCP in the SCI model group was significantly lower than that in the sham operation group (P<0.01); in contrast, the mRNA expression levels of ROCK II and RhoA in the SCI model group were markedly higher than those in the sham operation group (P<0.01). After treatment with EA or with the blocking agent Y27632, the mRNA expression levels of MLCP were not significantly higher than those in the SCI model group (P>0.05), and after treatment with EA plus the blocking agent Y27632, the MLCP mRNA expression level was significantly higher than that in the SCI model group (P<0.01). In contrast, the mRNA expression levels of RhoA and ROCK II were all significantly lower than

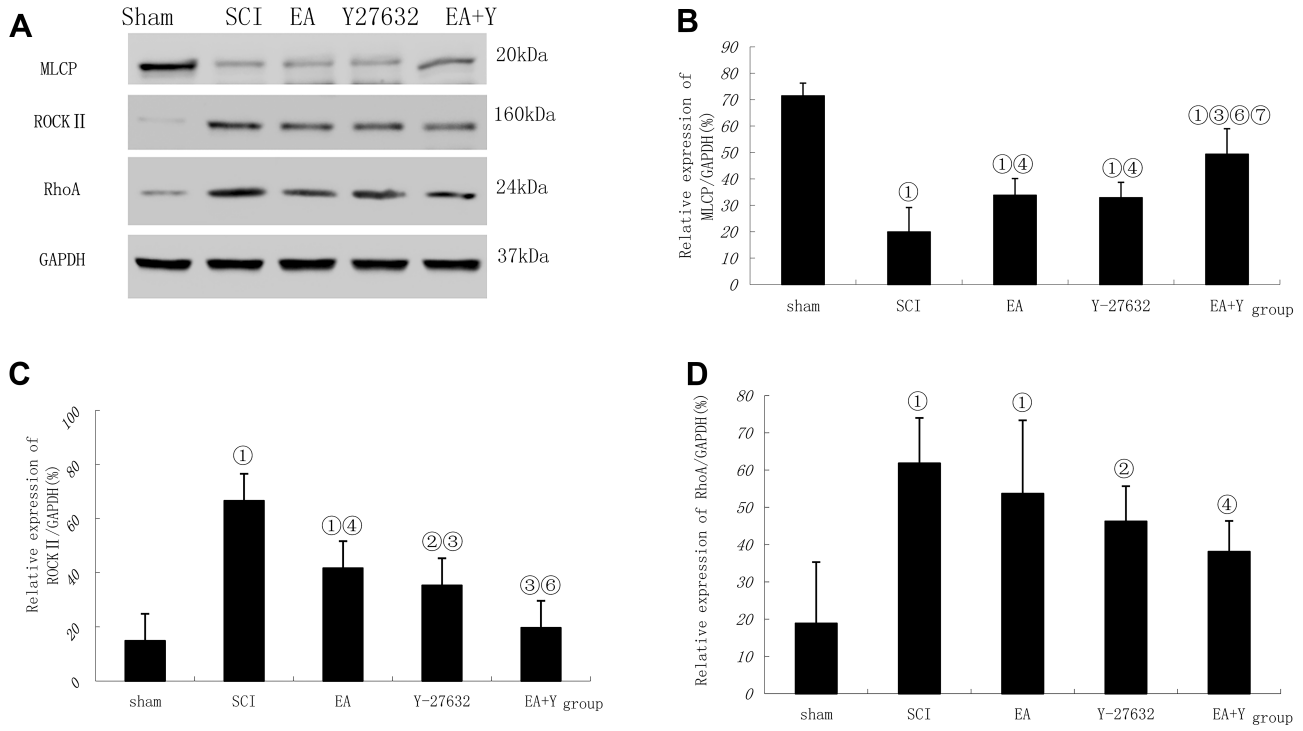

Figure 4 MLCP, ROCK II and RhoA activation following SCI. (**A**) Western blotting bands for MLCP, ROCK II, RhoA and GAPDH expression. Compiled results in a bar graph for the ratio (**B**) of MLCP/GAPDH expression. (**C**) of ROCK II/GAPDH expression. (**D**) of RhoA/GAPDH expression. ① P<0.01, ② P<0.05 versus sham. ③ P<0.01, ④ P<0.05 versus SCI. ⑥ P<0.05 versus EA. ⑦ P<0.01, ⑧P<0.05 versus Y27632. Data are shown as the mean±standard error of the mean (1-way analysis of variance and Student-Newman-Keuls post hoc test, n=4 rats/group).

Abbreviations: sham, sham operation; SCI, spinal cord injury; EA, electroacupuncture; Y, blocking agent Y27632; MLCP, myosin light chain phosphatase; ROCK II, Rho-associated kinase II; GAPDH, glyceraldehyde-3-phosphate dehydrogenase.

those in the SCI model group (P<0.01). Compared with EA treatment, in the blocking-agent-Y27632 treatment group, the mRNA expression of MLCP was not significantly increased (P>0.05); by contrast, the mRNA expression levels of RhoA and ROCK II were noticeably decreased (P<0.05 or <0.01) in the EA+Y group, and the mRNA expression of MLCP was significantly increased (P<0.01). The mRNA expression levels of ROCK II and RhoA were significantly decreased (P<0.01). Compared with Y27632 treatment, EA+Y treatment caused the mRNA expression of MLCP to significantly increase (P<0.01); by contrast, the mRNA expression levels of ROCK II and RhoA were not markedly decreased (P>0.05). The mRNA expression level was calculated using the $2^{-\Delta\Delta Ct}$ analytical method, as shown in Figure 5.

The Protein Expression of p-MYPT1 and MYPT1 by Western Blotting

The relative protein expression of p-MYPT1 in the SCI model group was noticeably higher than that in the sham operation group (P<0.01), and the ratio of p-MYPT1/MYPT1 had a similar profile to that of p-MYPT1 (P<0.01). By contrast, the expression of MYPT1 in the SCI model group was not significantly higher than that in the sham operation group (P>0.05). After treatment with EA or with the blocking agent Y27632 or with EA plus Y27632, the protein expression of p-MYPT1 and the ratio of p-MYPT1/MYPT1 were significantly lower than those in the SCI model group (P<0.01). The expression of MYPT1 was not significantly lower than that in the SCI model group (P>0.05). Except for the protein expression of p-MYPT1 in the EA +Y group, which was lower than that in the EA group, comparisons among EA, blocking agent Y27632 and EA plus Y27632 revealed no significant differences in the relative protein expression of p-MYPT1 and MYPT1 or the ratio of p-MYPT1/MYPT1 (P>0.05), as shown in Figure 6.

Caspase3 mRNA Expression by in situ Hybridization

In situ hybridization-positive cells contained brown spots or particles, as indicated by the arrows. In the sham operation group, rare expression of caspase3 was observed in the spinal cords of sham-operated rats. Injury induced increased

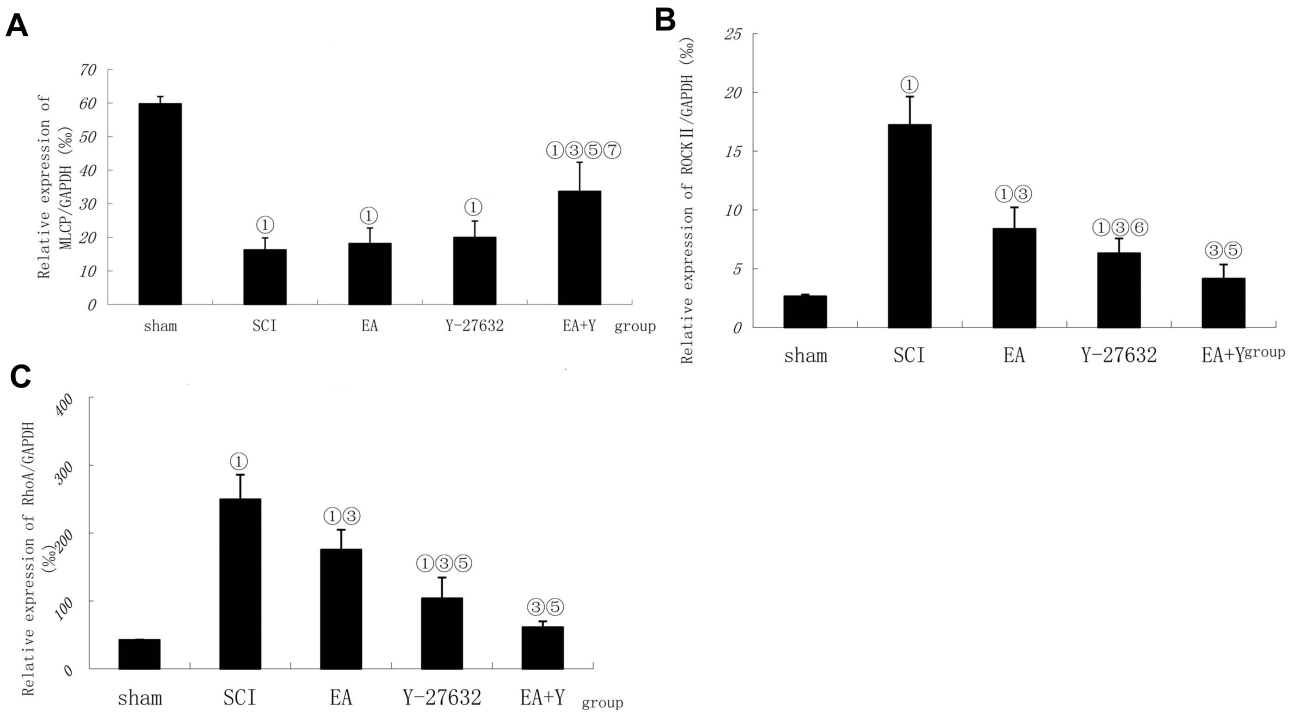

Figure 5 Effect of electroacupuncture on changes in mRNA expression of MLCP, ROCK II and RhoA in injured spinal cords. (**A**) Compiled results in a bar graph for MLCP expression. Compiled results in a bar graph (**B**) for ROCK II expression. (**C**) for RhoA expression.① P<0.01,. ③ P<0.01. ⑤ P<0.01; ⑥ P<0.05 versus EA. ⑦ P<0.01 versus Y27632. Data are expressed as the mean±SD (1-way analysis of variance and Student-Newman-Keuls post hoc test, n=4 rats/group).

Abbreviations: sham, sham operation; SCI, spinal cord injury; EA, electroacupuncture; Y, blocking agent Y27632; ROCK II, Rho-associated kinase II; MLCP, myosin light chain phosphatase.

caspase3 mRNA expression, and the number of caspase3 mRNA-positive cells in the SCI model group was significantly higher than that in the sham operation group (P<0.01). Treatment with EA or blocking agent Y27632 or EA plus blocking agent Y27632 decreased the mRNA expression of caspase3 (EA, Y27632, EA+Y), and the number of caspase3 mRNA-positive cells was significantly decreased compared with that in the SCI model group (P<0.01). Compared with EA treatment, treatment with blocking agent Y27632 or EA plus blocking agent Y27632(EA+Y) markedly decreased the caspase3 mRNA expression (P<0.01). The caspase3 mRNA-positive cell number in the EA+Y treatment group was not significantly decreased (P>0.05) compared with that in the blocking-agent-Y27632 treatment group, and the number of caspase3 mRNA-positive cells was also not significantly decreased (P>0.05), as shown in Figures 7 and 8.

Discussion

In this study, based on the Nogo/NgR and Rho/ROCK signaling pathway, we investigated the mechanism of EA treatment on SCI at the molecular level. The Rho/ROCK signaling pathway is influenced by the upstream Nogo/NgR signaling pathway and ultimately affects the growth of nerve axons through regulating its downstream substrate, MLC. Nogo-A is the most restrictive isomer in the Nogo family.[35] The signal of the extracellular myelin-related inhibitory factor is transmitted into the cell via the transmembrane protein NgR. The putative tripartite LINGO-1·p75 NTR·Nogo-66 receptor (NgR) complex, constituted by NgR, binds the synergistic receptor p75NTR and the common receptor LINGO-1 to activate the intracellular signal. LINGO-1 was originally identified as an essential component of a cell-surface receptor complex.[36] LINGO-1 is specifically expressed in oligodendroglial cells and nerve fibers in the nervous system and has significant inhibitory effects on the proliferation, maturation and myelination of oligodendroglial cells.[36]

In this study, after Western blotting and real-time fluorescence quantitative PCR detection, the mRNA and protein expression levels of Nogo-A, NgR and LINGO-1 were significantly increased in the SCI model group and were significantly higher than that in the sham operation group. After 14 days of EA treatment, the mRNA and protein expression levels of Nogo-A, NgR and LINGO-1 were significantly decreased. The results indicated that, after SCI, the expression of inhibitory signaling molecules

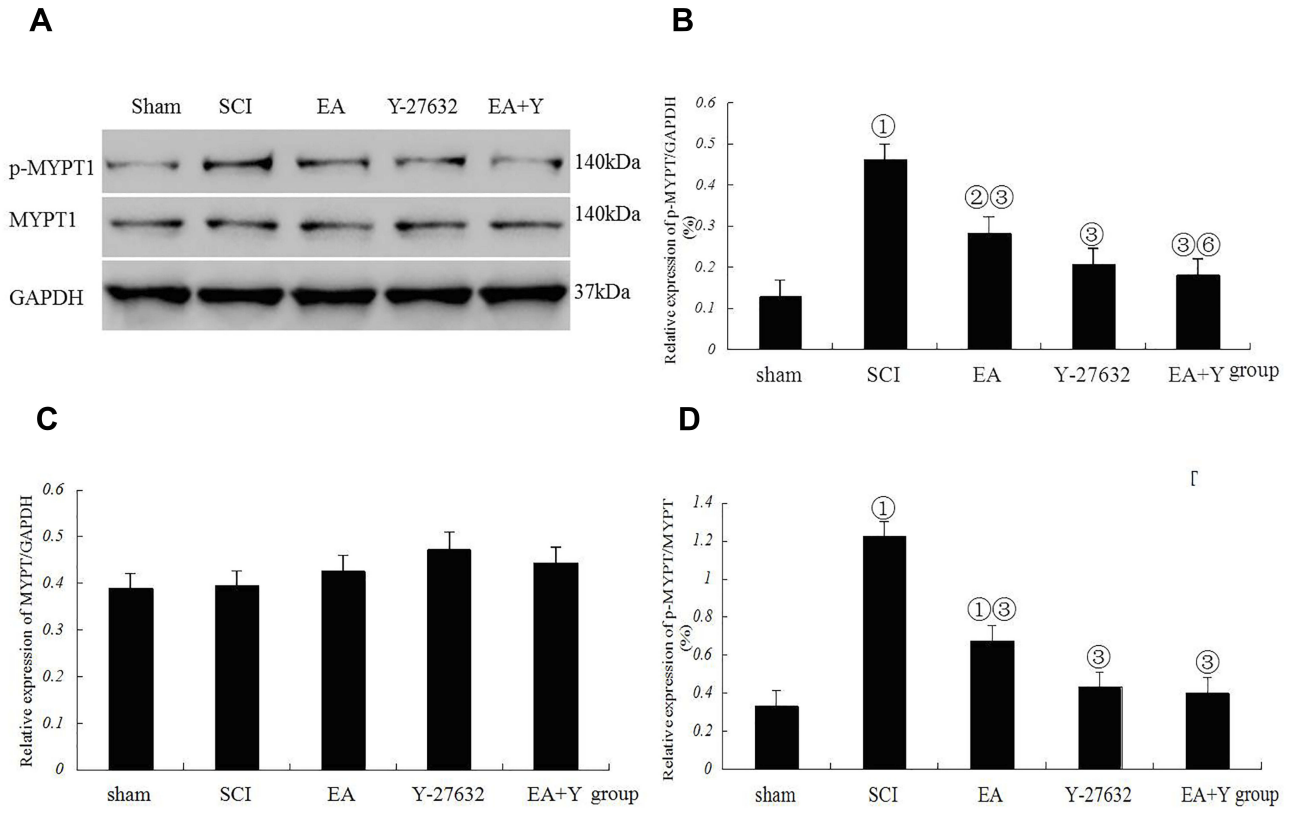

Figure 6 Myosin phosphatase target subunit 1 (MYPT1) activation following SCI. (**A**) Western blotting bands for phosphorylated MYPT1 (p-MYPT1), MYPT1, and GAPDH expression. Compiled results in a bar graph for the ratio (**B**) of p-MYPT1/GAPDH expression. (**C**) of MYPT1/GAPDH expression. (**D**) of p-MYPT1/MYPT1. ① p<0.01, ② P<0.05 versus sham. ③ P<0.01, ⑥ P<0.05 versus EA. Data are shown as the mean±standard error of the mean (1-way analysis of variance and Student-Newman-Keuls post hoc test, n=4 rats/group). sham: sham operation.

Abbreviations: SCI, spinal cord injury; EA, electroacupuncture; Y, blocking agent Y27632; MYPT1, myosin phosphatase target subunit 1; p-MYPT1, phosphorylated MYPT1; GAPDH, glyceraldehyde-3-phosphate dehydrogenase.

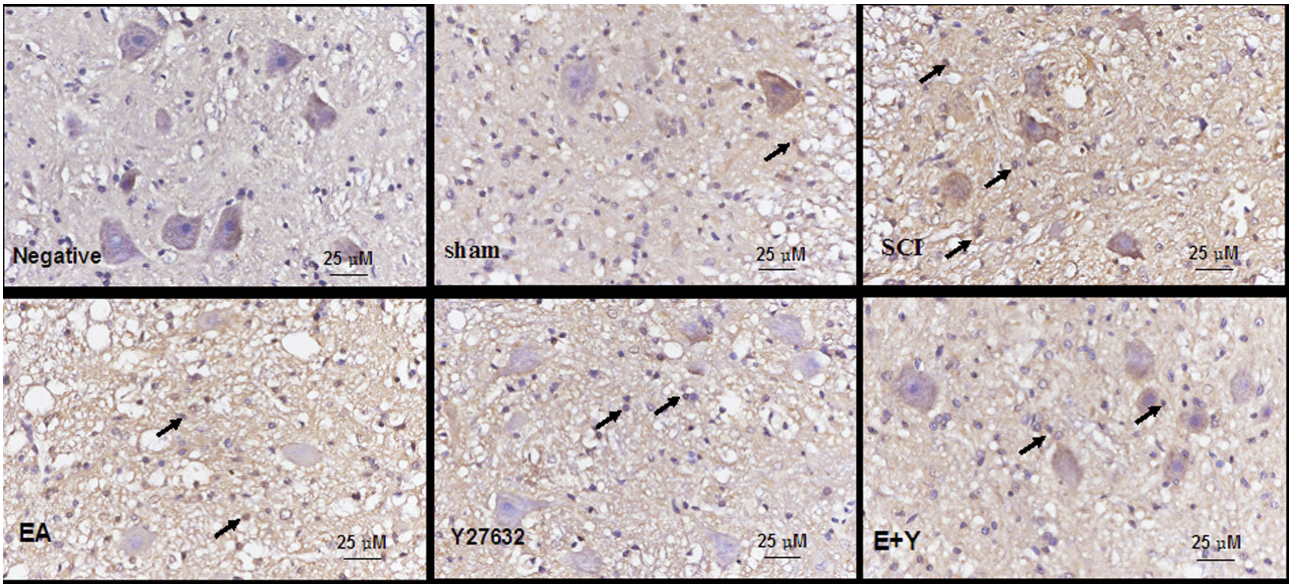

Figure 7 mRNA expression of caspase3 in injured spinal cords at 14 days following treatment (in situ hybridization, ×400). (Bar =25 μm).

Abbreviations: sham, sham operation; SCI, spinal cord injury; EA, electroacupuncture; Y, blocking agent Y27632.

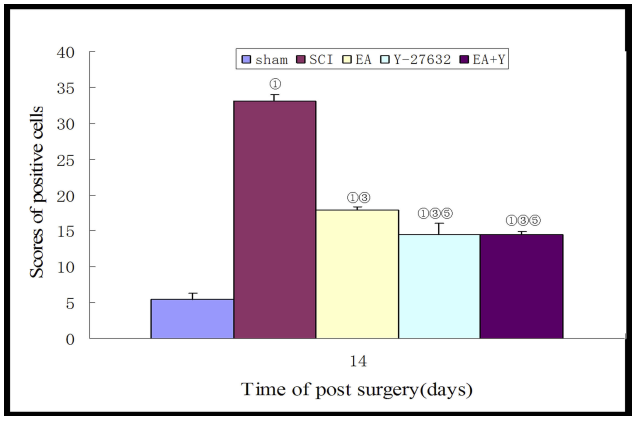

Figure 8 Compiled results in a bar graph for the number of caspase3 mRNA-positive cells. ① P<0.01. ③ P<0.01. ⑤ P<0.01 versus EA. Data are expressed as the mean±SD (1-way analysis of variance and Student-Newman-Keuls post hoc test, n=4 rats/group).
Abbreviations: sham, sham operation; SCI, spinal cord injury; EA, electroacupuncture; Y, blocking agent Y27632.

that affect the growth of nerve axons increased, while EA inhibited their increase. Li et al[37] found that at 1, 7, 14 and 28 days postsurgery, the expression of Nogo-A protein in spinal cord tissues that were located at the injury sites showed a tendency to increase and was strongest after 14 days. After treatment with EA, the Nogo-A expression decreased. Our previous study showed that the mRNA and protein expression of Nogo-A and NgR gradually increased from 1 day to 28 days postsurgery, and at the 21st day, the expression reached its peak[38]. The mRNA and protein expression of Nogo-A and NgR in the EA group treated for 14 days was lower than that in the SCI model group, and there was no significant difference between postoperative treatment for 7 days and treatment for 14 days.[38] In this study, the expression of LINGO-1 showed the same tendency as Nogo-A and NgR did.[26] Mi et al[17] found that 14 days after injury, LINGO-1 mRNA expression levels increased to approximately 5-fold higher than that of normal animals. In addition, the expression of LINGO-1 was upregulated in the spinal cord axons of rats after SCI and white matter lesions of multiple sclerosis (MS). Lv et al[39] proved that the treatment of intrathecal injection with a high-titer rabbit LINGO-1 antiserum in an SCI animal model group could increase the survival of neurons near the SCI area.

RhoA and its downstream effector Rho kinase (ROCK) control and regulate cytoskeleton dynamics. The RhoA/Rho kinase pathway regulates a wide range of fundamental cell functions, including contraction, motility, proliferation, gene expression, and apoptosis.[40] The key molecules in the Rho/ROCK signaling pathway involve Rho, ROCK, MYPT1 and MLCP. RhoA is a major isomer of the Rho family, and ROCK II is one of the most important Rho downstream effector molecules, which are preferentially found in the brain, spinal cord, and muscle.[20,41,42] In this study, the mRNA and protein expression levels of RhoA and ROCK II were high in the SCI model group and were significantly higher than that in the sham operation group. Separate treatment with EA or blocking agent Y27632 significantly reduced the mRNA and protein expression of ROCK II and the mRNA expression of RhoA, and the two methods of treatment had a synergistic effect. The combination of the two methods significantly reduced the expression of RhoA protein. This result was similar to our previous findings showing that EA significantly reduces the mRNA and protein expression of RhoA and ROCK II.[28] In addition, Dubreuil et al[43] found that four to fourteen days after contusion SCI, the signal intensity of RhoA mRNA was significantly higher in spinal cord segments below the injury site than in segments above the injury site.

After being activated, ROCKII can phosphorylate Thr696 and Thr853 in MYPT-1, a target subunit of MLCP, and then, MYPT-1 becomes modified to p-MYPT1, which inactivates MLCP, thus resulting in an increase in the level of MLC phosphorylation, i.e., p-MLC, thereby affecting the actin system and causing collapse of the axon growth cone, apoptosis, and finally inhibiting axon growth.[44,45] Detection by Western blotting and real-time quantitative PCR revealed that the mRNA and protein expression of MLCP decreased in the SCI model group and was significantly lower than that in the sham operation group. Separate treatment with EA or blocking agent Y27632 significantly increased the expression of MLCP protein but had little effect on the expression of MLCP mRNA. The combination of EA and blocking agent Y27632 significantly increased the mRNA and protein expression of MLCP. In this study, we found that p-MYPT1 was significantly increased in the SCI model group and was significantly higher than that in the sham operation group, and the ratio of p-MYPT1/MYPT1 was also markedly higher than that in the sham operation group; by contrast, the expression of MYPT1 showed no obvious changes between the two groups. Separate treatment with EA or blocking agent Y27632 or treatment with a combination of EA and blocking agent Y27632 significantly decreased the expression of p-MYPT1 protein and the ratio of p-MYPT1/MYPT1, but had little effect on the expression of MYPT1 protein. The above results have the same trendency with the p-MLC and MLC in our previous study.[31]

The effect of EA on SCI was achieved by downregulating the expression of related axonal growth-inhibiting factors, such as Nogo-A, NgR, LINGO-1, ROCK II, RhoA and MYPT1 mentioned above, reducing the inflammatory response, such as cPLA2, PGE2, etc.[29] and decreasing apoptosis,[46] ultimately promoting the recovery of lower limb movement function. Caspase3, known as cysteine protease 32(CPP32), is a major effector of caspase. Caspase3, also known as death executioner protease, is a common downstream effector of a variety of apoptotic pathways and plays a central role in the apoptosis process.-[47] This study showed that, injury induced caspase3 mRNA expression increased, and the number of positive cells in the SCI model group was significantly higher than that in the sham operation group, after treatment with EA or blocking agent Y27632 alone or with a combination of EA and blocking agent Y27632, the mRNA expression of caspase3 significantly decreased. BBB scores indicated that after 14 days of treatment, compared with the SCI model group, the treatment groups showed significantly increased BBB scores, and there was no significant difference between the EA treatment group and the Y27632 treatment group, but the BBB score in the combination EA+Y27632 treatment group was higher than those in the EA group and Y27632 group. These results showed that both EA treatment and Y27632 treatment promoted the regeneration of injured nerves and improved the activity of the hind limbs of rats. Furthermore, EA +Y27632 treatment was superior to the single-treatment method. This result was consistent with our above research regarding the effect of EA plus blocking agent Y27632 on the Rho/ROCK signal pathway.

Studies have shown that the Rho/ROCK signaling pathway can also regulate cytoplasmic phospholipase A2 (cPLA2) and promote the inflammatory response, which could lead to neurocyte damage and apoptosis.[48,49] Acupuncture is used to treat diseases through multiple targets and multiple pathways. Based on the Nogo/NgR and Rho/ROCK signaling pathway, this study offers a research direction for further exploration of EA. Through the regulation of the inflammatory response and cell apoptosis, EA might get the beneficial effect in the treatment of SCI. This article provides an experimental basis for the clinical application of EA treatment for SCI.

Acknowledgments

Professor Jian-ming WAN in Jiangxi University of Traditional Chinese Medicine provides the guidance of animal model building and the equipment of electric Cortical Contusion Impactor. This work was supported by the National Natural Science Foundation of China (No. 81360562), and the National Key Research Projects of China (No. 2018YFC1707700).

Disclosure

The authors report no conflicts of interest in this work.

References

1. Yoshimura T, Arimura N, Kaibuchi K. Molecular mechanisms of axon specification and neuronal disorders. *Ann N Y Acad Sci*. 2006;1086:116–125. doi:10.1196/annals.1377.013
2. Gao J, Cheng LH, Min YJ. Clinical Research in acupuncture treating the recovery period of spinal cord injury. *Anmo Yu Kangfu*. 2015;6:18–21.
3. Gao LJ, Sun YC, Li JJ, Bai F, Li PK. Effects of electroacupuncture in different time on variations of fractional anisotropy mean value of diffusion tensor tractography in spinal cord injured rats. *Zhongguo Kangfulilun Yu Shijian*. 2014;20:728–733.
4. Min YJ, Cheng LH, Yao HH, Yang L, Min ZY, Pei J. Effect of Santong electroacupuncture on expression of p75 neurotrophin receptor in rats with spinal cord injury. *Zhongguo Kangfulilun Yu Shijian*. 2017;23:621–627.
5. Lee BB, Cripps RA, Fitzharris M, Wing PC. The global map for traumatic spinal cord injury epidemiology: update 2011, global incidence rate. *Spinal Cord*. 2014;52:110–116. doi:10.1038/sc.2012.158
6. New PW, Baxter D, Farry A, Noonan VK. Estimating the incidence and prevalence of traumatic spinal cord injury in Australia. *Arch Phys Med Rehabil*. 2015;96:76–83. doi:10.1016/j.apmr.2014.08.013
7. Burke DA, Linden RD, Zhang YP, Maiste AC, Shields CB. Incidence rates and populations at risk for spinal cord injury: A regional study. *Spinal Cord*. 2001;39:274–278. doi:10.1038/sj.sc.3101158
8. Rabchevsky AG, Patel SP, Springer JE. Pharmacological interventions for spinal cord injury: where do we stand? How might we step forward?. *Pharmacol Ther*. 2011;132:15–29. doi:10.1016/j.pharmthera.2011.05.001
9. Wang ZQ, Min YJ. Observation of effect on thermal moxibustion treatment of incomplete spinal cord injury urinary retention. *Chengdu Zhongyiyao Daxue Xuebao*. 2013;36:60–63.
10. Wang WC, Lu JC, Wang Q, et al. Effect on the activities of daily life of the patients with traumatic spinal cord injury treated by the paraplegia-triple-needling method. *Zhongguo Zhenjiu*. 2012;32:877–881.
11. Paola FA, Arnold M. Acupuncture and spinal cord medicine. *J Spinal Cord Med*. 2003;26:12–20. doi:10.1080/10790268.2003.11753654
12. Min YJ, Cheng LH, Gao J. Comparative observations on three-unblocking acupuncture for the treatment of spinal cord injury in convalescent patients with paraplegia. *Shanghai Zhenjiu*. 2013;32:1010–1013.
13. Min ZY, Cheng LH, Min YJ. Research progress of Nogo/NgR pathway in spinal cord nerve regeneration. *Jiangxi Zhongyiyao Daxue Xuebao*. 2016;28:103–106.
14. Ding LQ, He XW, Min YJ. Advances in the Study of Rho/Rock pathway in axonal regeneration after spinal cord injury. *Shanghai Zhenjiu Zazhi*. 2015;34:1246–1248.
15. Liu BP, Cafferty WB, Budel SO, Strittmatter SM. Extracellular regulators of axonal growth in the adult central nervous system. *Philos Trans R Soc Lond B Biol Sci*. 2006;361:1593–1610.
16. Wang KC, Kim JA, Sivasankaran R, Segal R, He Z. P75 interacts with the Nogo receptor as a co-receptor for Nogo, MAG and OMgp. *Nature*. 2002;420:74–78. doi:10.1038/nature01176

17. Mi S, Lee X, Shao Z, et al. LINGO-1 is a component of the Nogo-66 receptor/p75 signaling complex. *Nat Neurosci*. 2004;7:221–228. doi:10.1038/nn1188
18. Park JB, Yiu G, Kaneko S, et al. A TNF receptor family member, TROY, is a coreceptor with Nogo receptor in mediating the inhibitory activity of myelin inhibitors. *Neuron*. 2005;45:345–351. doi:10.1016/j.neuron.2004.12.040
19. Bito H, Furuyashiki T, Ishihara H, et al. A critical role for a Rho-associated kinase, p160ROCK, in determining axon outgrowth in mammalian CNS neurons. *Neuron*. 2000;26:431–441. doi:10.1016/S0896-6273(00)81175-7
20. Erschbamer MK, Hofstetter CP, Olson L. RhoA, RhoB, RhoC, Rac1, Cdc42, and Tc10 mRNA levels in spinal cord, sensory ganglia, and corticospinal tract neurons and long-lasting specific changes following spinal cord injury. *J Comp Neurol*. 2005;484:224–233. doi:10.1002/(ISSN)1096-9861
21. Kubo T, Endo M, Hata K, et al. Myosin IIA is required for neurite outgrowth inhibition produced by repulsive guidance molecule. *J Neurochem*. 2008;105:113–126. doi:10.1111/j.1471-4159.2007.05125.x
22. Madura T, Yamashita T, Kubo T, Fujitani M, Hosokawa K, Tohyama M. Activation of Rho in the injured axons following spinal cord injury. *EMBO Rep*. 2004;5:412–417. doi:10.1038/sj.embor.7400117
23. Dickson BJ. Rho GTPases in growth cone guidance.Curr. *Opin Neurobiol*. 2001;11:103–110. doi:10.1016/S0959-4388(00)00180-X
24. Monnier PP, Sierra A, Schwab JM, Henke-Fahle S, Mueller BK. The Rho/ROCK pathway mediates neurite growth-inhibitory activity associated with the chondroitin sulfate proteoglycans of the CNS glial scar. *Mol Cell Neurosci*. 2003;22:319–330. doi:10.1016/S1044-7431(02)00035-0
25. Huang YZ, Feng DX, Li J, Kang JP, Ye F. In vitro effect of Y27632 on dorsal root ganglion neurons axonal regeneration in neogenetic rats with spinal cord injury. *Zhongguo Jizhu Jisui Zazhi*. 2010;20:765–770.
26. Min ZY, Cheng LH, Min YJ. Effect of electroacupuncture on Nogo/NgR signal pathway related factors in spinal cord injury rats. *Beijing Zhongyiyao Daxue Xuebao*. 2016;39:926–932.
27. Min YJ, Zhang H, Xiao WP. Experimental study of electroacupuncture on mRNA and protein expression of Nogo-A and NgR in SCI rats. *Shizhen Guoyi Guoyao*. 2017;28:995–998.
28. Min YJ, Ding LL, Cheng LH, et al. Effect of electroacupuncture on the mRNA and protein expression of Rho-A and Rho-associated kinase II in spinal cord injury rats. *Neural Regen Res*. 2017;12:276–282. doi:10.4103/1673-5374.200811
29. Liu NK, Deng LX, Zhang YP, et al. Cytosolic phospholipase A2 protein as a novel therapeutic target for spinal cord injury. *Ann Neurol*. 2014;75:644–658. doi:10.1002/ana.24134
30. Shi SH, Yin MX, Song M, Song JL, Zheng GH, Li ZG. Experimental study on the expression of Nogo-A after spinal cord injury in rats. *Shanxi Zhongyi*. 2010;31:371–373.
31. Hong ES, Yao HH, Min YJ, et al. The mechanism of electroacupuncture for treating spinal cord injury rats by mediating Rho/Rho-associated kinase signaling pathway. *JSCM*. 2019 doi:10.1080/10790268.2019.1665612.
32. Gao J, Zhang YJ, Min YJ, Cui J. Study and application of acupoints in the treatment of paraplegia. *Jiangxi Zhongyiyao*. 2013;44:54–56.
33. Min YJ, Deng L, Hong ES. Orthogonal study on different acupuncture factors based on hypothalamic- pituitary-adrenal axis in rats with kindey Yang deficiency. *Shanghai Zhenjiu Zazhi*. 2016;35:339–343.
34. Zhang L, Ni YQ, Li YF. Ligustrazine facilitates hair cell regeneration in the cochlea following gentamicin ototoxicity. *Neural Regen Res*. 2010;5:735–740.
35. Chong SY, Rosenberg SS, Fancy SP, et al. Neurite outgrowth inhibitor Nogo-A establishes spatial segregation and extent of oligodendrocyte myelination. *Proc Natl Acad Sci USA*. 2012;109:1299–1304. doi:10.1073/pnas.1113540109
36. Meabon JS, De Laat R, Ieguchi K, Wiley JC, Hudson MP, Bothwell M. LINGO-1 protein interacts with the p75 neurotrophin receptor in intracellular membrane compartments. *J Biol Chem*. 2015;290:9511–9520. doi:10.1074/jbc.M114.608018
37. Li ZP, Kong KM, Chen YC, Guo TM, Chen ZF, Liu JB. Effect of electroacupuncture on the expression of Nogo-A protein in rats with spinal cord injury. Shantou Daxue Yixueyuan Xuebao. 2008;21:129–133.
38. Min YJ, Sun J, Jia YZ, et al. Phased expression of gene and protein of Nogo-A and NgR in rats with spinal cord injury and time window of electroacupuncture. Zhongguo Kangfu Lilun Yu Shijian. 2018;24:621–628.
39. Lv J, Xu RX, Jiang XD, et al. Passive immunization with LINGO-1 polyclonal antiserum afforded neuroprotection and promoted functional recovery in a rat model of spinal cord injury. Neuroimmuno modulation. 2010;17:270–278. doi:10.1159/000290043.
40. Loirand G, Guérin P, Pacaud P. Rho kinases in cardiovascular physiology and pathophysiology. *Circ Res*. 2006;98:322–334. doi:10.1161/01.RES.0000201960.04223.3c
41. Chen XL, Liu L, Wen QQ, et al. Effect of acupuncture at different acupoints on RhoA/ROCK signaling pathway in gastric antral smooth muscle tissue of rats with diabetic gastroparesis. *Shijie Huaren Xiaohua Zazhi*. 2016;24:3508–3516.
42. Wu XF, Chen XL, Zheng XN, et al. Effect of Different Stimulating Strength of Electroacupuncture on Gastrointestinal Motility and RhoA/ROCK Signaling in Gastric Antral Smooth Muscle in Diabetic Gastroparesis Rats. *Zhen Ci Yan Jiu*. 2018;43:169–174. doi:10.13702/j.1000-0607.170299
43. Dubreuil CI, Winton MJ, McKerracher L. Rho activation patterns after spinal cord injury and the role of activated Rho in apoptosis in the central nervous system. *J Cell Biol*. 2003;162:233–243. doi:10.1083/jcb.200301080
44. Khasnis M, Nakatomi A, Gumpper K, Eto M. Reconstituted human myosin light chain phosphatase reveals distinct roles of two inhibitory phosphorylation sites of the regulatory subunit, MYPT1. *Biochemistry*. 2014;53:2701–2709. doi:10.1021/bi5001728
45. Khromov A, Choudhury N, Stevenson AS, Somlyo AV, Eto M. Phosphorylation- dependent autoinhibition of myosin light chain phosphatase accounts for Ca2+ sensitization force of smooth muscle contraction. *J Biol Chem*. 2009;284:21569–21579. doi:10.1074/jbc.M109.019729
46. Hu HL, Huang XL, Liu F, Quan RF. Advances in experimental studies on the mechanism of huatuo jiaji (Ex-B2) point acupuncture treatment for spinal cord injury. *Shanghai Zhenjiu Zazhi*. 2016;35:1480–1483.
47. Odonkor CA, Achilefu S. Modulation of effector caspase cleavage determines response of breast and lung tumor cell lines to chemotherapy. *Cancer Invest*. 2009;27(4):417–429. doi:10.1080/07357900802438585
48. Wu X, Walker CL, Lu Q, et al. RhoA/Rho Kinase Mediates Neuronal Death Through Regulating cPLA2 Activation. *Mol Neurobiol*. 2017;54:6885–6895. doi:10.1007/s12035-016-0187-6
49. Zhang RN, Chai Z, Fan HJ, et al. Preventive and therapeutic effect and its mechanism of Wuzi Yanzong Pills on EAE mouse. *Zhonghua Zhongyiyao*. 2018;33:1316–1319.